Check for updates

Trimerization and cyclization of reactive P-functionalities confined within OCO pincers†

Beatrice L. Chinen,[a] Jakub Hyvl, [ID][a] Daniel F. Brayton,[a] Matthew M. Riek,[a] Wesley Y. Yoshida,[a] Timothy W. Chapp,[b] Arnold L. Rheingold[c] and Matthew F. Cain [ID] *[a]

In order to stabilize a 10–P–3 species with C_{2v} symmetry and two lone pairs on the central phosphorus atom, a specialized ligand is required. Using an NCN pincer, previous efforts to enforce this planarized geometry at P resulted in the formation of a C_s-symmetric, 10π-electron benzazaphosphole that existed as a dynamic "bell-clapper" in solution. Here, OCO pincers **1** and **2** were synthesized, operating under the hypothesis that the more electron-withdrawing oxygen donors would better stabilize the 3-center, 4-electron O–P–O bond of the 10–P–3 target and the sp^3-hybridized benzylic carbon atoms would prevent the formation of aromatic P-heterocycles. However, subjecting **1** to a metalation/phosphination/reduction sequence afforded cyclotriphosphane **3**, resulting from trimerization of the P(I) center unbound by its oxygen donors. Pincer **2** featuring four benzylic CF_3 groups was expected to strengthen the O–P–O bond of the target, but after metal–halogen exchange and quenching with PCl_3, unexpected cyclization with loss of CH_3Cl was observed to give monochlorinated **5**. Treatment of **5** with $(p\text{-}CH_3)C_6H_4MgBr$ generated crystalline P-(p-Tol) derivative **6**, which was characterized by NMR spectroscopy, elemental analysis, and X-ray crystallography. The complex ^{19}F NMR spectra of **5** and **6** observed experimentally, were reproduced by simulations with MestreNova.

Introduction

Transition metal (TM) catalysis[1] has revolutionized the chemical industry, enabling the conversion of cheap feedstocks into valuable products for pharmaceuticals, polymers, and other specialty chemicals.[2] However, some of the most commonly employed metals like Ru,[3] Rh,[4] Ir,[5] Pd,[6] and Pt[7] are scarce, while the supporting ligands are often phosphines,[8] N-heterocyclic carbenes (NHCs),[9] and/or other elaborate scaffolds including chiral diols,[10] functionalized cyclopentadienyl ligands (*ansa*-metallocenes),[11] and rare and/or non-naturally occurring amines.[12] These metal–ligand platforms are both expensive and toxic, resulting in a delicate balance between the benefits of chemical synthesis and its harmful effects to the environment and human health. An environmentally friendly and sustainable TM alternative would be to use a more benign and earth-abundant Main Group (MG) element such as phosphorus as the active center. Yet, unlike TMs that have closely spaced HOMO–LUMO gaps, MG compounds feature

orbitals that are far apart energetically, which limits their ability to engage in TM-type reactivity like oxidative addition, insertion, and reductive elimination.[13] Fortunately, by distorting phosphines away from their classic three-fold symmetry, their frontier orbitals can become energetically accessible.[14] For example, C_s-symmetric phosphorus triamide **A** can promote oxidative addition of alcohols and amines.[15–17] Related C_{2v}-symmetric **B**,[18] describable by numerous resonance structures including **B′** and **B″** due to extensive conjugation within the ONO ligand[19] will oxidatively add H_2 from H_3N–BH_3 and transfer that hydrogen equivalent to azobenzene in a catalytic fashion, producing hydrazines (Fig. 1).[20]

Resonance structure **B″** is a T-shaped 10–P–3 species,[21] which contains a frontier orbital environment remarkably similar to a C_{2v}-symmetric, d^8 ML_3 TM complex like the Ir(PCP) pincer fragment with a low-lying σ acceptor orbital and a higher energy lone pair with π-symmetry,[22] capable of engaging in backbonding to an incoming substrate (Fig. 2). In the case of Ir(PCP) pincers,[23] this results in the oxidative addition of dihydrogen,[24] alkanes,[25] and ammonia.[26] However, **B** does not add H_2 because the high-energy p-lone pair necessary for backbonding is delocalized into the ligand scaffold.[27] Therefore, we speculated that replacing the tridentate ONO ligand with a traditional pincer featuring a central aryl donor would prevent π-delocalization, rendering the p lone pair available for backbonding to small molecules.

In 2010,[28] the Dostál group demonstrated that heavier, C_{2v}-symmetric 10–Bi–3 species **C** (Scheme 1, inset) could be stabilized within an NCN pincer and similar analogues could

[a] Department of Chemistry, University of Hawai'i at Mānoa, 2545 McCarthy Mall, Honolulu, HI 96822, USA. E-mail: mfcain@hawaii.edu

[b] Department of Chemistry, Allegheny College, 520 N. Main Street, Meadville, PA 16335, USA

[c] Department of Chemistry, University of California, 9500 Gilman Drive, La Jolla, San Diego, California 92093, USA
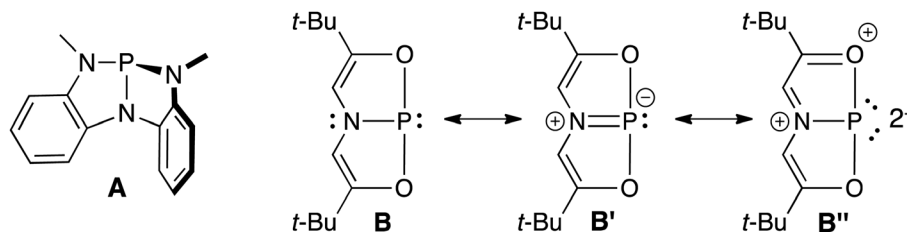
Fig. 1 Structures of geometrically distorted **A** and **B** with contributing resonance structures **B′** and **B″**.
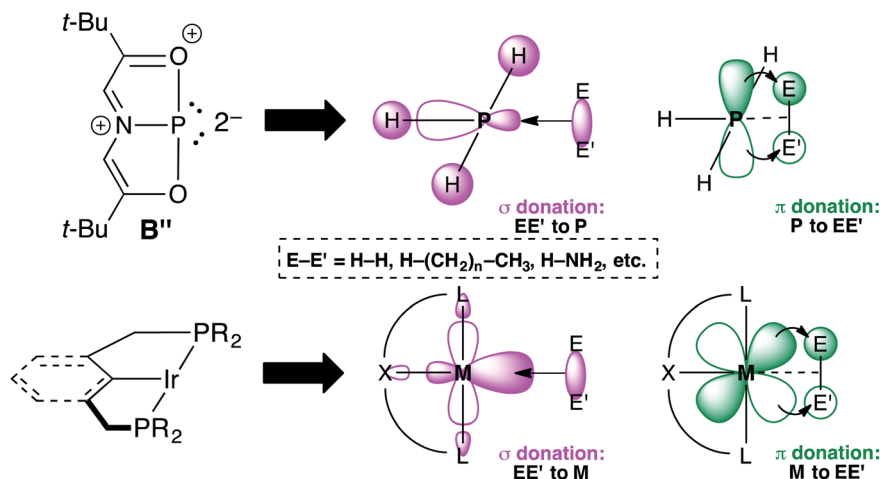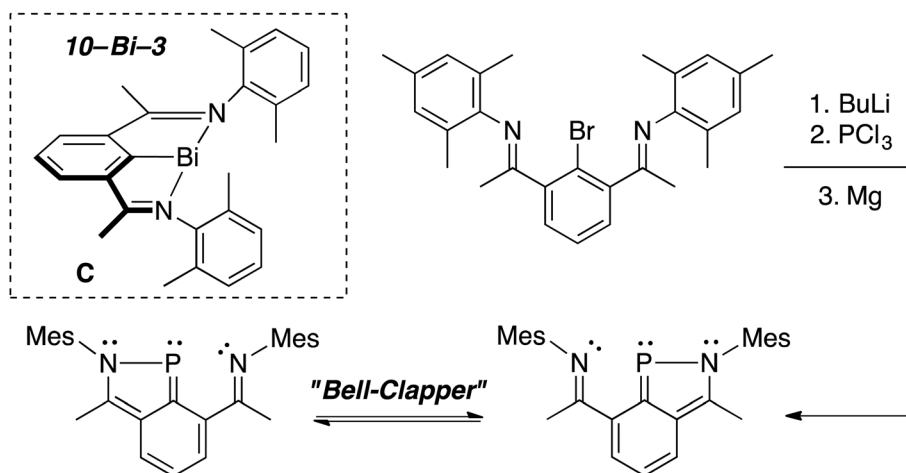

Fig. 2 Simplified frontier orbital comparison between **B″** and an Ir(PCP) pincer fragment.

perform oxidative addition of the weak bonds of diphenyldichalcogenides[29] (ex. PhS–SPh, S–S bond = 55 kcal mol^{-1}).[30] This led us to attempt to stabilize a 10–P–3 species within a related NCN scaffold with the hope that substrates with stronger bonds, like those present in dihydrogen (H–H bond = 104 kcal mol^{-1}),[31] could be broken at P. Yet, unlike the Bi analogue, reduction of the P(III) intermediate did not afford the desired 10–P–3 species, but rather a C_s-symmetric 10π-electron

benzazaphosphole with a tethered imine arm, which existed as a dynamic "bell-clapper" in solution (Scheme 1).[32]

In order to access the targeted 10–P–3 species, we hypothesized that strengthening the 3-center, 4-electron bond between the axial donors and phosphorus (indicated in red, Chart 1, left) could be accomplished using more electron-withdrawing oxygen atoms.[19] Additionally, sp^3-hybridized benzylic carbons would be employed on the pincer arms to prevent the formation of aromatic P-heterocycles.[33] Guided by these ligand design

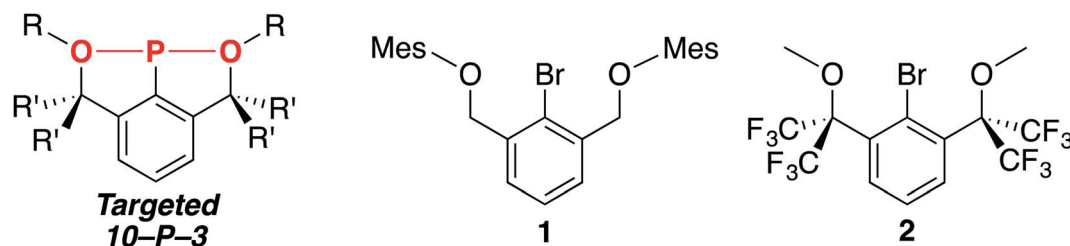**Scheme 1** Synthesis of a benzazaphosphole "bell-clapper" with 10−Bi−3 species **C** shown in the inset.

Chart 1 The targeted 10−P−3 species and brominated OCO pincers **1** and **2**.

principles, brominated OCO pincers **1** (ref. 34) and **2** were synthesized (Chart 1, right), and we report here on the unexpected trimerization and cyclization chemistry encountered when installing the P-functionality within these scaffolds.

Results and discussion

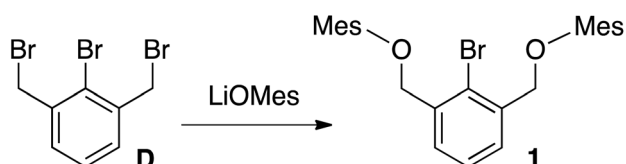### Synthesis of 1 and the formation of cyclotriphosphane 3 *via* reduction

Tribromide **D** [35] was treated with LiOMes (Mes = 2,4,6-trimethylbenzene), generated *in situ* from BuLi and 2,4,6-trimethylphenol, affording **1** in 64% yield (Scheme 2).

Monobrominated OCO pincer **1** was readily identified by ^{1}H NMR spectroscopy with its downfield shifted benzylic signals (CDCl$_3$: δ 4.93; relative to **D**, CDCl$_3$: δ 4.55), integrating in a 4 : 2 : 1 ratio with the diagnostic doublet/triplet pattern of the central aryl protons. The proligand was further characterized by ^{13}C{^{1}H} NMR spectroscopy and elemental analysis, and its structure was unequivocally confirmed by X-ray crystallography (Fig. 3).

Based on literature precedent with heavier pnictogens,[28,36] it was anticipated that the bromide in **1** could be substituted by a PCl$_2$ unit *via* a lithium–halogen exchange/phosphination

sequence. Reduction of the intermediate dichlorophosphine would then produce the desired 10–P–3 species. However, treatment of **1** with BuLi, followed by quenching with PCl$_3$ and reduction[37] with PMe$_3$ did not afford the target, but rather cyclotriphosphane **3** in 56% yield (Scheme 3). The ^{31}P{^{1}H} NMR spectrum of **3** (inset) contained upfield shifted resonances at −116 and −144 ppm with a J_{PP} = 186 Hz, consistent with a solution structure in which two P atoms are spectroscopically distinct from a third.[38] This NMR signature is in line with other (PR)$_3$ species like (PIs)$_3$ (Is = 2,4,6-tri-isopropylbenzene) and (PMes)$_3$,[38] but not diphosphenes like Mes*P=PMes* (Mes* = 2,4,6-tri-*tert*-butylbenzene), which feature *bona fide* P=P double bonds (2.034(2) Å),[39] downfield shifted ^{31}P{^{1}H} NMR signals (δ = 493),[40] and if unsymmetrical,[38,40] large J_{PP} couplings approaching 600 Hz (Mes*P=PMes, J_{PP} = 571 Hz). Other higher order monocyclophosphanes like tetrameric [P(*t*-Bu)]$_4$ are singlets (^{31}P NMR: δ −57.8),[41] while (PR)$_5$ pentamers (R = Ph) are complex multiplets (^{31}P NMR: δ −3)[42] (Scheme 3, bottom panel).

The structure of cyclotriphosphane **3** was further corroborated by ^{1}H and ^{13}C{^{1}H} NMR spectroscopy. Specifically, this "2-Down, 1-Up"-type (referring to the organic substituents on P) structure was readily apparent as two distinct aryl *O*-Mes singlets were observed in the ^{1}H NMR spectrum (CDCl$_3$) at 6.71 and 6.62 ppm in an 8 : 4 ratio with all the remaining resonances paired (although some broadened) in a similar 2 : 1 fashion. In addition, the ^{13}C{^{1}H} NMR spectrum displayed two separate benzylic signals and four methyl signals, all consistent with the assignment of **3**. Ultimately, the structure of **3**, as proposed, was established by X-ray crystallography (Fig. 4). Structural characterization of cyclotriphosphanes is rare,[43] but the bond lengths and angles of **3** are quite similar to [P(*t*-Bu)]$_3$ and

Scheme 2 Synthesis of **1**.
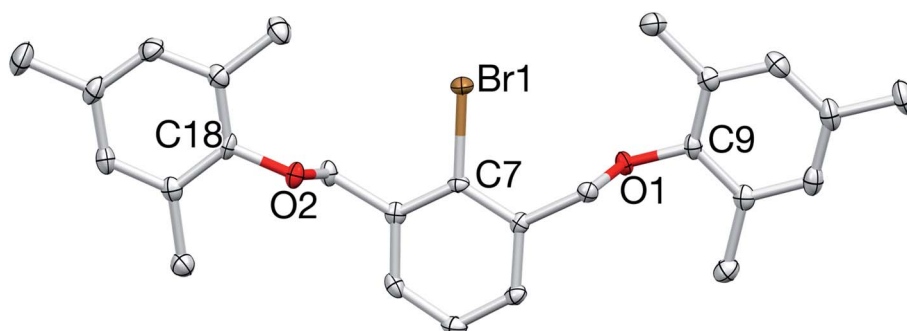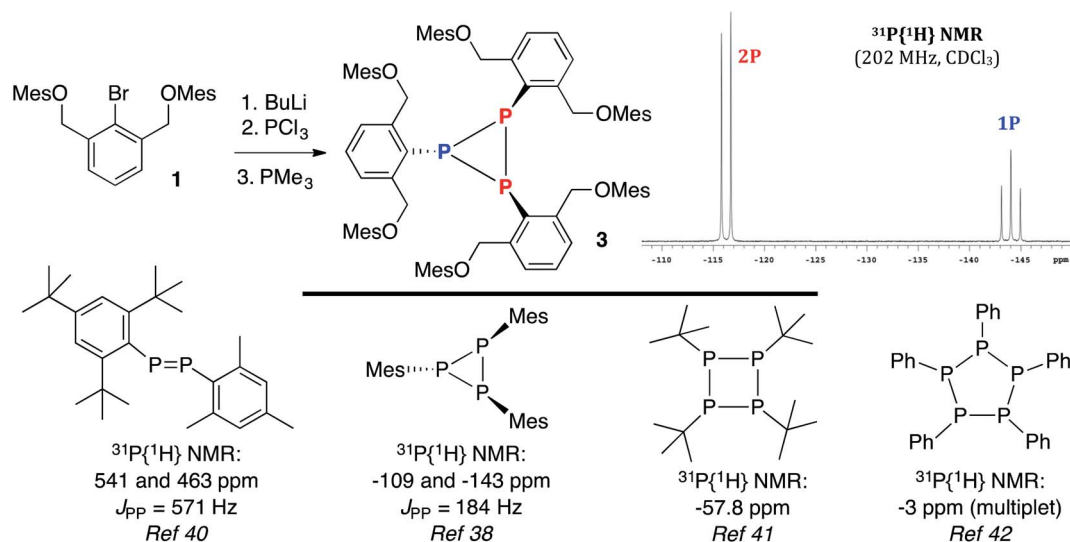

Fig. 3 X-ray crystal structure of **1**. All bond lengths (Å) and angles (deg) can be found in the ESI.†

Scheme 3 Synthesis of **3** and a selected view of its $^{31}P\{^1H\}$ NMR spectrum (top) and related $(RP)_n$ oligomers (bottom).

$[PCH(SiMe_3)_2]_3$.[44,45] In particular, the P–P bonds measure 2.217(2), 2.194(2), and 2.237(2) Å, respectively with PPP angles of 60.95(7), 59.02(7), and 60.03(7) deg, indicative of P–P single bonds and unhybridized P-centers confined into a small ring system.[43] The P–C bonds in **3** (avg = 1.847 Å) are slightly shorter than observed with $[P(t\text{-Bu})]_3$ and $[PCH(SiMe_3)_2]_3$, which may be due to the presence of an sp^2-hybridized[46] C-substituent with considerably less bulk and more flexibility than the t-Bu and

$CH(SiMe_3)_2$ groups. In fact, in comparison with cyclotriphosphanes $[P(t\text{-Bu})]_3$, $[PCH(SiMe_3)_2]_3$, $(PIs)_3$, and $(PMes)_3$, it is somewhat surprising that **3** adopts a related structure because normally, as steric bulk decreases, the size of the oligomeric fragment increases (note: $(PMes)_3$ *versus* $(PPh)_5$); however, here, many close contacts (under 4 Å)[47] between the aryl rings of the OMes units may impart added stability to the cyclotriphosphane structure.

Fig. 4 X-ray crystal structure of **3**. Selected bond lengths (Å) and angles (deg): P_1–P_2 = 2.194(2), P_2–P_3 = 2.217(2), P_1–P_3 = 2.237(2), P_1–C_1 = 1.839(5), P_2–C_{27} = 1.853(5), P_3–C_{53} = 1.850(5), P_3–P_2–P_1 = 60.95(7), P_1–P_3–P_2 = 59.02(7), P_3–P_1–P_2 = 60.03(7).

Scheme 4 Synthesis of **2**.

Regardless, the structure of **3** suggested that the axial 3-center, 4-electron bond of the targeted 10–P–3 species was still the weak point. In fact, cyclotriphosphane **3** is formally the result of trimerization[48] of an OCO-supported P(ɪ) intermediate after the *O*-donors rotated away from the electron-deficient phosphorus center. In order to elucidate any mechanistic details, the phosphination and reduction steps (shown in Scheme 3) were monitored by $^{31}P\{^1H\}$ NMR spectroscopy, but did not reveal the generation of RP=PMe$_3$ (R = OCO pincer), a proposed precursor to the formation of cyclotriphosphanes such as (PIs)$_3$, nor did a solution of **3**, PMe$_3$, and benzaldehyde produce any phosphaalkenes.[48]

Synthesis of 2 and cyclization of PCl$_2$-functionalized 4

In order to further strengthen the 3-center, 4-electron O–P–O bond of the potential 10–P–3 species, the electronegativity of the *O*-donors was increased using benzylic CF$_3$ groups. To this end, diol **E**,[49] now accessible in a single step[50] from dimethyl 2-bromoisophthalate and TMSCF$_3$ and previously used to stabilize numerous hypervalent MG species[51] including 10–Br–3 (ref. 52) and 12–I–5,[49] was selected as the building block to brominated OCO pincer **2**. After isolation of **E** in multi-gram quantities,[53] dimethylation with MeI/K$_2$CO$_3$ in DMF resulted in the isolation of **2** in 78% yield (Scheme 4).

The ^1H NMR spectrum (CDCl$_3$) featured a prominent singlet for the OMe groups at 3.52 ppm, which integrated in a 6 : 2 : 1 ratio with the remaining central aryl protons, while the ^{19}F NMR spectrum contained a single resonance at −66.9 ppm, all consistent with the expected C_{2v} symmetry of **2**. Additional characterization by $^{13}C\{^1H\}$ NMR spectroscopy, elemental analysis, and X-ray crystallography confirmed its structure (Fig. 5).

Cognizant that lithium–halogen exchange using BuLi in the presence of fluorine atoms may be complicated by LiF formation[54] and that magnesium–halogen exchange is faster with electron-withdrawing substrates and more functional group tolerant,[55] **2** was exposed to i-PrMgCl·LiCl,[56] resulting in smooth *in situ* conversion to the Grignard reagent, which was subsequently quenched with a precooled solution (−35 °C) of PCl$_3$ in THF (Scheme 5).

The reaction mixture was then analyzed by $^{31}P\{^1H\}$ NMR spectroscopy (THF), revealing the presence of some unreacted PCl$_3$ (218 ppm), (i-Pr)PCl$_2$ (202 ppm), and an unidentified product (171 ppm). The ^{19}F NMR spectrum (C$_6$D$_6$) displayed four complex multiplet CF$_3$ signals at −68.9, −70.4, −73.4, and −76.3 ppm, demonstrating that the unidentified product no longer contained C_{2v} symmetry and was not PCl$_2$-substituted **4**. Instead, we suspected an intramolecular reaction occurred between the highly electrophilic PCl$_2$ functionality and one of the *O*-donors, resulting in cyclization and the loss of chloride, which subsequently dealkylated[57] the O–Me unit affording monochlorinated **5**. Using MestreNova,[58] simulated ^{19}F NMR signals of **5** that closely matched the experimental spectrum were generated (Fig. 6), revealing the presence of both second order and long range coupling between the diastereotopic CF$_3$ groups, the heterocyclic P atom, and the aryl protons (see ESI† for details).
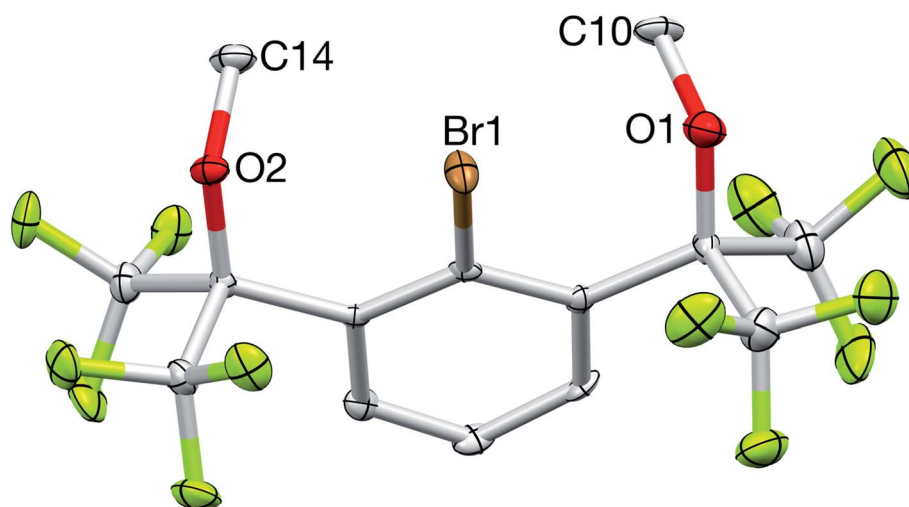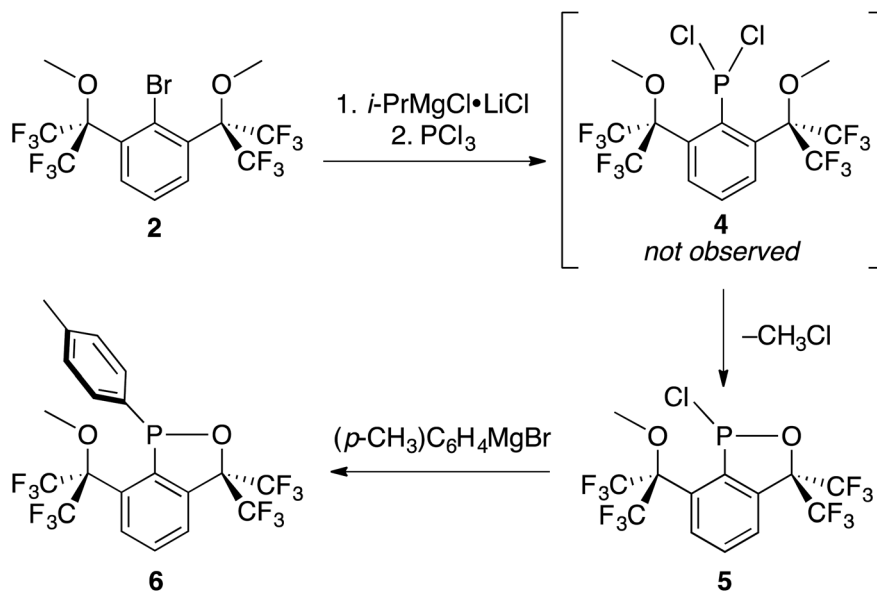

Fig. 5 X-ray crystal structure of **2**. All bond lengths (Å) and angles (deg) can be found in the ESI.†

Scheme 5 Intramolecular cyclization of **4** to **5** and synthesis of crystalline derivative **6**.

Experimentally, the cyclization to **5** was confirmed by synthesizing a more crystalline derivative *via* nucleophilic substitution. Specifically, a solution of **5** in THF at 0 °C was treated with $(p\text{-CH}_3)\text{C}_6\text{H}_4\text{MgBr}$, leading to the isolation of **6** as large off-white crystals in 38% yield (from **2**, Scheme 5, above; see Fig. 9 for picture of crystals). The $^{31}\text{P}\{^1\text{H}\}$ NMR spectrum (C_6D_6) of **6** exhibited an apparent septet at 129.7 ppm ($^4J_{\text{PF}} = 6$ Hz), while its ^{19}F NMR spectrum, like **5**, displayed four distinct

resonances for the diastereotopic CF_3 groups at −69.5, −69.6, −74.0, and −76.5 ppm. These complex ^{19}F NMR signals could also be reproduced with MestreNova (Fig. 7, see ESI† for details).

^1H NMR spectroscopy (C_6D_6) further corroborated the structure of **6** as the aromatic signals associated with the *p*-tolyl group and the three inequivalent protons of the central aryl unit of the OCO pincer integrated in a 2 : 2 : 1 : 1 : 1 ratio; in
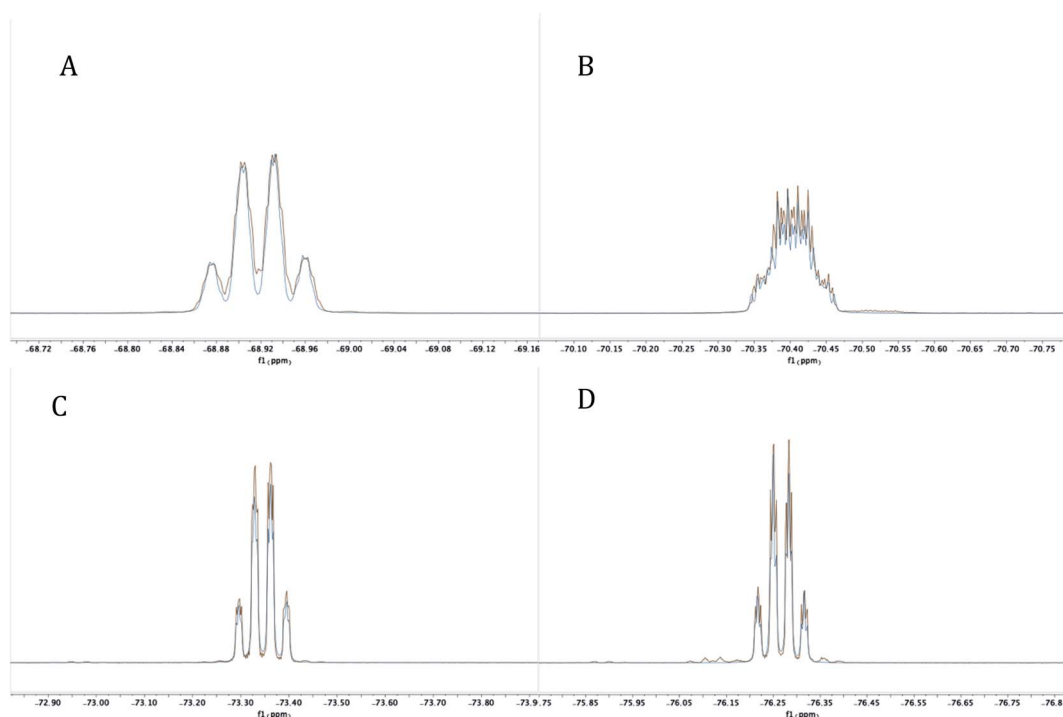

Fig. 6 Experimental (red) and simulated (blue) ^{19}F NMR signals at −68.9237 (A), −70.4093 (B), −73.3518 (C) and −76.2722 (D) for **5** at 282 MHz.
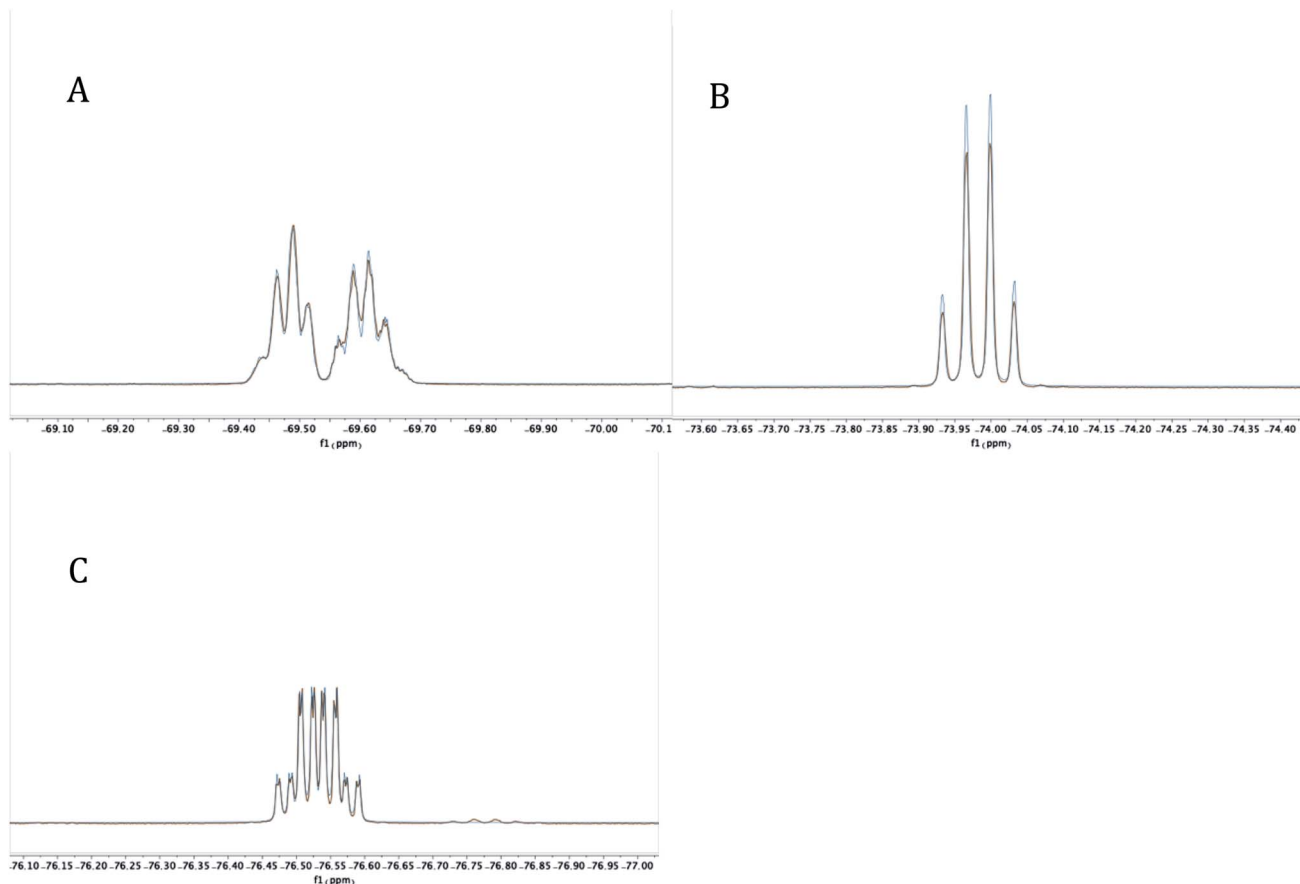
Fig. 7 Experimental (red) and simulated (blue) ^{19}F NMR signals at −69.4819 and −69.6176 (A), −73.9876 (B), and −76.5368 (C) for **6** at 282 MHz.

addition, two distinct methyl signals (OMe, 3.11 ppm and *p*-Me, 1.92 ppm) were observed. The ^{13}C{^{1}H} NMR spectrum also highlighted the inequivalency of the CF$_3$ groups with four overlapping signals (see ESI† for zoomed in NMR spectrum): two quartets ($J_{CF} \sim 290$ Hz) combined with two quartets of doublets ($J_{CF} \sim 290$ Hz and $J_{CP} \sim 9$ or 2 Hz, respectively) in the 122–123 ppm range, while the two quaternary carbons C(CF$_3$)$_2$ resonated as a septet (80.8 ppm,

$J_{CF} = 28$ Hz) and a septet of doublets (89.5 ppm, $J_{CF} = 31.5$ Hz, $J_{CP} = 16.5$ Hz, Fig. 8).

Ultimately, although disordered across a pseudo mirror plane, X-ray crystallography established the structure of **6** with its bulk purity verified by elemental analysis (Fig. 9).
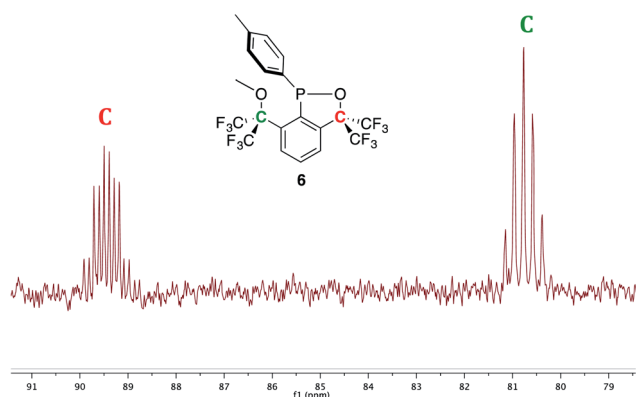

Fig. 8 A selected view of the ^{13}C{^{1}H} NMR spectrum (C$_6$D$_6$) of **6** displaying the quaternary carbons.
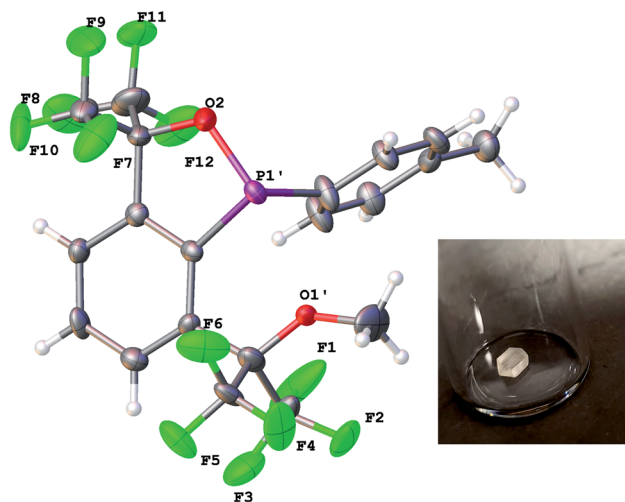

Fig. 9 X-ray crystal structure of **6**. All bond lengths (Å) and angles (deg) can be found in the ESI.† A picture of one of the large blocks is shown in the inset.

Unfortunately though, like **1**, fluorinated OCO pincer **2** also failed to deliver access to the 10–P–3 target. Here, the increased electron-withdrawing power of four benzylic CF₃ groups resulted in, after a metal–halogen exchange/phosphination sequence, highly reactive dichlorophosphine **4**, which *via* an unexpected cyclization[57] to **5**, partially disassembled the pincer framework before reduction could be attempted.

Conclusions and future directions

Undoubtedly, the hypothesis (*vide supra*) that the formation of 10–P–3 species over benzazaphosphole "bell-clappers" would be favored by switching from NCN pincers to more electron withdrawing OCO pincers with sp³-hybridized benzylic carbon atoms was overly simplistic. As the phrase goes, "hindsight is 20/20" and here, the biggest oversight was expecting a P-center to adopt a high-energy planarized geometry when lower barrier pathways to phosphorus maintaining its preferred pyramidal geometry exist. For example, 10–P–3 species like B'' (Fig. 1) and the target (Chart 1, left) can be considered "internally-solvated phosphinidenes"[19] that are supported by a 3-center, 4-electron O–P–O bond. However, B'' features a conjugated ONO ligand that locks the *O*-donors into place, while C_{Ar}–C_{sp^3} or C_{sp^3}–O bond rotations within OCO pincer **1** expose the reactive P(ɪ) center, resulting in oligomerization chemistry,[43,48,59] a known route by which phosphorus preserves its pyramidal structure and is exemplified by the formation of trimer **3**. To prevent this, we aimed to strengthen the 3-center, 4-electron bond using more electron-withdrawing *O*-donors, but neglected how the enhanced electrophilicity of PCl₂-substituted **4** can make the ligand framework susceptible to nucleophilic attack, in this case, cyclization to **5** (and its functionalization to **6**). Guided by these lessons, a pincer framework that is rigid featuring electron-withdrawing *O*-donors, but lacking sp³-hybridized[57] carbon atoms prone to nucleophilic attack may provide the stabilization necessary to confine a P-center into a planarized 10–P–3 arrangement and will be investigated.

Experimental section

General experimental details

Unless otherwise specified, all reactions were performed under an atmosphere of nitrogen in an MBraun or Vacuum Atmospheres glovebox or using standard Schlenk techniques. All glassware was dried overnight in an oven at 140 °C prior to use. Solvents used in the glove box were purchased directly from chemical suppliers (Aldrich or Acros), pumped directly into the glove box, and stored over oven-activated 4 or 5 Å molecular sieves (Aldrich). Solvents used outside the glove box were purged with N₂ for 30 min and stored over molecular sieves. TMSCF₃ was dried by cryogenic transfer. ¹H, ¹³C{¹H}, ¹⁹F, and ³¹P{¹H} NMR spectra were recorded on a Varian Mercury-300 (300/75/282/121 MHz), Varian Unity Inova-500 (500/126/470/202 MHz), or Agilent 600 DD2 (600/151/565/243 MHz) spectrometer at ambient temperature. Chemical shifts are reported in ppm downfield of tetramethylsilane using the solvent as internal standard (¹H CDCl₃ = 7.27 ppm, ¹H C₆D₆ = 7.16 ppm,

¹³C CDCl₃ = 77.16 ppm, ¹³C C₆D₆ = 128.06 ppm). Multiplicities are abbreviated as br (broad), s (singlet), d (doublet), t (triplet), q (quartet), or m (multiplet). Coupling constants (J) are reported in Hertz (Hz). Flash column chromatography was performed on silica gel (40–63 μm, SiliCycle). High-resolution mass spectrometry (HRMS) was recorded on an Agilent 6545 LC-MS Q-ToF spectrometer (NSF-1532310). Dimethyl 2-bromoisophthalate and [Me₄N][F] were synthesized according to the published procedures.[60,61] All other chemicals were used as received, unless otherwise noted.

Synthesis of 1

In the glovebox, 2,4,6-trimethylphenol (3.00 g, 22.03 mmol, 2.5 equiv.) was dissolved in THF (100 mL), and a 1.6 M solution of *n*-BuLi in hexanes (13.0 mL, 20.8 mmol, 2.3 equiv.) was added dropwise at room temperature. The reaction mixture was stirred for 15 min. Subsequently, tribromide **D** (3.086 g, 9.0 mmol) was added to the stirred solution, and the reaction mixture was transferred to a Schlenk bomb equipped with a Teflon screw cap and heated at 100 °C for 1 day. The volatiles were then removed under reduced pressure, and the crude residue was extracted with a toluene : hexane mixture (1 : 1, 3 × 15 mL). The combined extracts were filtered through a Celite plug, and the filtrate was concentrated under vacuum then purified by column chromatography (silica gel, toluene : hexane 1 : 1, R_f = 0.63). The title product (2.64 g, 5.822 mmol) was obtained as white plates in 65% yield. X-Ray quality crystals were obtained by slow evaporation from a concentrated solution of **1** in *n*-hexanes.

Anal. Calcd for C₂₆H₂₉BrO₂: C, 68.87; H, 6.45. Found: C, 68.77; H, 6.27. ¹H NMR (500 MHz, CDCl₃): δ 7.78 (d, J = 7.6 Hz, 2H, Ar), 7.51 (t, J = 7.6 Hz, 1H, Ar), 6.89 (s, 4H, Ar), 4.93 (s, 4H, CH₂), 2.30 (s, 12H, Me), 2.29 (s, 6H, Me). ¹³C{¹H} NMR (126 MHz, CDCl₃): δ 153.5 (Ar), 137.8 (Ar), 133.6 (Ar), 130.9 (Ar), 129.6 (Ar), 127.9 (Ar), 127.7 (Ar), 121.6 (Ar), 73.3 (CH₂), 20.9 (CH₃), 16.4 (CH₃).

Synthesis of 2

Diol **E** (3.61 g, 7.38 mmol) and DMF (180 mL) were combined in a Schlenk flask with a stir bar. The solution was purged with N₂ on the Schlenk line for 30 min, then K₂CO₃ (5.10 g, 36.9 mmol, 5 equiv.) was added with stirring under positive N₂ pressure. Next, MeI (2.30 mL, 36.9 mmol, 5 equiv.) was injected *via* syringe, and the reaction mixture was stirred overnight, then quenched with NH₄Cl (aq) and extracted with toluene (3 × 50 mL). The combined organic layers were washed with water, brine, dried over MgSO₄, filtered, and the filtrate concentrated under vacuum, resulting in pale yellow solid **2** (2.97 g, 5.74 mmol, 78%). Recrystallization from acetonitrile (8 mL) at 4 °C afforded crystals suitable for X-ray diffraction.

Anal. Calcd for C₁₄H₉BrO₂F₁₂: C, 32.52; H, 1.75. Found: C, 32.71; H, 1.77. ¹H NMR (500 MHz, CDCl₃): δ 7.76 (d, J = 10 Hz, 2H, Ar), 7.51 (t, J = 10 Hz, 1H, Ar), 3.52 (s, 6H, Me). ¹³C{¹H} NMR (151 MHz, CDCl₃): δ 134.1 (Ar), 129.6 (Ar), 127.0 (Ar), 123.5 (Ar), 122.4 (q, J = 290 Hz, CF₃), 86.5 (septet, J = 29 Hz, C(CF₃)₂), 54.8 (OMe). ¹⁹F NMR (471 MHz, CDCl₃): δ −66.9 (s).

Synthesis of 3

OCO-supported aryl bromide **1** (1.134 g, 2.50 mmol) was loaded into a Schlenk flask, dissolved in Et_2O (60 mL), taken outside of the glovebox, and cooled to -78 °C. A 1.6 M solution of *n*-BuLi in hexanes (1.7 mL, 2.72 mmol, 1.1 equiv.) was injected (under N_2), and the reaction mixture was stirred at -78 °C for 5 min. A second Schlenk flask containing a solution of PCl_3 (550 mg, 4.01 mmol, 1.6 equiv.) in Et_2O (5 mL) was transferred *via* cannula to the cooled reaction mixture. The reaction mixture was stirred at -78 °C for 10 min and then at room temperature (RT) for 1 h, leading to the precipitation of a white solid. The volatiles were removed under reduced pressure, the Schlenk flask was brought back into the glovebox, the residue was triturated with Et_2O (10 mL), and the volatiles were again removed. The residue was dissolved in THF (20 mL), and PMe_3 was added (485 mg, 6.375 mmol, 2.6 equiv.). The reaction mixture was stirred at RT for 1 day. The organic volatiles were removed under reduced pressure, and the residue was extracted with toluene (3 × 20 mL). The combined extracts were filtered through a Celite plug, the filtrate was concentrated to dryness, triturated with *n*-pentane (10 mL), and again concentrated to dryness under reduced pressure. The resulting residue was triturated with acetonitrile (10 mL) and stirred at RT for 1 h, generating a white precipitate that was collected by filtration and dried (565 mg, 0.466 mmol, 56%). X-Ray quality crystals of **3** were obtained by recrystallization from a solution of hot acetonitrile.

Anal. Calcd for $C_{78}H_{87}O_6P_3$: C, 77.20; H, 7.23. Found: C, 76.89; H, 7.14. $^{31}P\{^1H\}$ NMR (202 MHz, $CDCl_3$): δ -116.2 (d, $^1J_{PP}$ = 186 Hz), -144.0 (t, $^1J_{PP}$ = 186 Hz). ^1H NMR (500 MHz, $CDCl_3$): δ 7.71 (d, J = 7.7 Hz, 2H, Ar^1), 7.40 (t, J = 7.7 Hz, 1H, Ar^1), 7.33–7.28 (m, 4H, Ar^2), 7.28–7.22 (m, 2H, Ar^2), 6.71 (s, 8H, Ar^2), 6.62 (s, 4H, Ar^1), 5.39 (s, 4H, CH_2–Ar^1), 4.71 (br, 8H, CH_2–Ar^2), 2.25 (s, 12H, Ar^1), 2.20 (s, 6H, Ar^1), 2.02 (s, 12H, Ar^2), 1.95 (br, 24H, Ar^2). ^{13}C NMR (126 MHz, $CDCl_3$): δ 153.46 (Ar), 153.44 (Ar), 143.5 (Ar), 143.4 (d, J_{PC} = 6.9 Hz, Ar), 133.6 (Ar), 133.0 (Ar), 132.9 (Ar), 130.7 (Ar), 130.5 (Ar), 130.4 (Ar), 129.6 (Ar), 129.4 (Ar), 129.0 (Ar), 128.4 (d, J_{PC} = 10.0 Hz, Ar), 127.9 (Ar), 126.4 (Ar), 73.2 (CH_2), 72.8 (d, J_{PC} = 7.6 Hz, CH_2), 20.9 (CH_3), 16.7 (CH_3), 16.4 (CH_3), 16.3 (CH_3).

Synthesis of 6

Fluorinated aryl bromide **2** (500 mg, 0.967 mmol) was dissolved in 6 mL of THF in a vial with a stir bar inside the glovebox and (i-Pr)MgCl·LiCl was added dropwise *via* syringe (0.82 mL, 1.064 mmol, 1.1 equiv., 1.3 M in THF), resulting in a homogeneous, yellow reaction mixture. The reaction mixture was stirred for 1 h at room temperature (RT) then directly filtered into 2 mL of a pre-cooled solution (-35 °C, 1 h) of PCl_3 (146 mg, 1.064 mmol, 1.1 equiv.) in THF. The solution was warmed to RT for 1 h then analyzed by $^{31}P\{^1H\}$ NMR spectroscopy, revealing the presence of unreacted PCl_3 (218 ppm), i-$PrPCl_2$ (202 ppm) and the chlorophosphine (170 ppm). The "intermediate" product mixture was then concentrated under vacuum to remove the volatile and unwanted phosphorus byproducts (PCl_3 and i-$PrPCl_2$), leaving a pale yellow residue that was dissolved in

6 mL of THF and transferred to a Schlenk bomb fitted with a screw-top Teflon cap. The bomb was taken outside of the glovebox, cooled to 0 °C, and (p-CH_3)C_6H_4MgBr (1.06 mL, 1.064 mmol, 1.1 equiv., 1.0 M in THF) was injected *via* syringe under positive N_2 pressure, affording a light orange reaction mixture, which was subsequently warmed to RT. The Schlenk bomb was resealed (under positive N_2 pressure), brought back inside the glove box, and an aliquot was analyzed by $^{31}P\{^1H\}$ NMR spectroscopy displaying a prominent signal at 129 ppm with slight impurities at -2 and -8 ppm. The entire reaction mixture was concentrated under vacuum, extracted with pentane (3 × 50 mL), and filtered through a Kimwipe plug. The filtrate was concentrated under vacuum, dissolved in ether (2 mL) and cooled to -35 °C overnight, resulting in large white/colorless blocks suitable for X-ray diffraction (202 mg, 0.371 mmol, 38% yield).

Anal. Calcd for $C_{20}H_{13}F_{12}O_2P$: C, 44.14; H, 2.41. Found: C, 44.09; H, 2.41. ^1H NMR (600 MHz, C_6D_6): δ 7.57 (br d, J = 8 Hz, 1H, Ar), 7.52 (d, J = 8 Hz, 1H, Ar), 7.10 (apparent t, J = 8 Hz, 2H, Ar), 6.88 (t, J = 8 Hz, 1H, Ar), 6.81 (d, J = 8 Hz, 2H, Ar), 3.11 (s, 3H, OMe), 1.92 (s, 3H, *p*-Me). $^{13}C\{^1H\}$ NMR (151 MHz, C_6D_6): δ 143.4 (d, J = 33 Hz, Ar), 141.2 (Ar), 137.8 (d, J = 41 Hz, Ar), 135.7 (d, J = 6 Hz, Ar), 133.0 (d, J = 5 Hz, Ar), 132.2 (d, J = 25 Hz, Ar), 131.1 (Ar), 130.0 (Ar), 129.0 (d, J = 8 Hz, Ar), 126.9 (Ar), four overlapping CF_3 signals*: 123.1 (qd, $J \sim$ 290 and 9 Hz), 123.0 (q, $J \sim$ 290 Hz), 122.5 (q, $J \sim$ 290 Hz), and 122.4 (qd, $J \sim$ 290 and 3 Hz), 89.5 (septet of doublets, J = 31.5 and 16.5 Hz, $C(CF_3)_2$ in P-ring), 80.8 (septet, J = 28 Hz, $C(CF_3)_2$), 55.3 (OMe), 21.2 (Me). ^{19}F NMR (282 MHz, C_6D_6):** δ -69.5 (m, $J_{FF} \sim$ 8 Hz, $J_{PF} \sim$ 2 Hz, $J_{HF} \sim$ 0.5–2 Hz), -69.6 (m, $J_{FF} \sim$ 8 Hz, $J_{PF} \sim$ 7 Hz, $J_{HF} \sim$ 0.5–2.5 Hz), -74.0 (m, $J_{FF} \sim$ 9 Hz, $J_{HF} \sim$ 0.5–1 Hz), and -76.5 (m, $J_{FF} \sim$ 9 Hz, $J_{HF} \sim$ 1–5 Hz). $^{31}P\{^1H\}$ NMR (121 MHz, C_6D_6): δ 129.4 (septet, J = 6 Hz). *In $CDCl_3$, the overlapping CF_3 signals in the $^{13}C\{^1H\}$ NMR spectrum are better resolved: δ 122.5 (q, J = 290 Hz), 122.3 (qd, J = 290 and 9 Hz), 122.0 (q, J = 290 Hz), 121.6 (qd, J = 290 and 2 Hz). **Reported coupling constants in the ^{19}F NMR spectrum were determined by simulation with Mestrenova.

Experimental NMR spectra, simulated ^{19}F NMR spectra using MestreNova, and X-ray crystallography

See the ESI† for details.

Conflicts of interest

There are no conflicts to declare.

Acknowledgements

Notes and references

1 J. F. Hartwig, *Organotransition Metal Chemistry: From Bonding to Catalysis*, University Science Books, 2010.

2 K. Weissermel and H.-J. Arpe, *Industrial Organic Chemistry*, VCH, Weinheim, 1997.

3 Selected examples: (*a*) C. Gunanathan and D. Milstein, Bond Activation and Catalysis by Ruthenium Pincer Complexes, *Chem. Rev.*, 2014, **114**, 12024–12087; (*b*) N. Uematsu, A. Fujii, S. Hashiguchi, T. Ikariya and R. Noyori, Asymmetric Transfer Hydrogenation of Imines, *J. Am. Chem. Soc.*, 1996, **118**, 4916–4917.

4 Selected examples: (*a*) I. D. Gridnev, M. Yasutake, T. Imamoto and I. P. Beletskaya, Asymmetric Hydrogenation of α,β-Unsaturated Phosphonates with Rh-BisP* and Rh-MiniPHOS Catalysts: Scope and Mechanism of the Reaction, *Proc. Natl. Acad. Sci. U.S.A.*, 2004, **101**, 5385–5390; (*b*) R. Noyori, M. Kitamura and T. Ohkuma, Toward Efficient Asymmetric Hydrogenation: Architectural and Functional Engineering of Chiral Molecular Catalysts, *Proc. Natl. Acad. Sci. U.S.A.*, 2004, **101**, 5356–5362.

5 Selected examples: (*a*) J. Choi, A. H. R. MacArthur, M. Brookhart and A. S. Goldman, Dehydrogenation and Related Reactions Catalyzed by Iridium Pincer Complexes, *Chem. Rev.*, 2011, **111**, 1761–1779; (*b*) R. H. Crabtree and M. W. Davis, Directing Effects in Homogeneous Hydrogenation with [Ir(cod)(PCy₃)(py)]PF₆, *J. Org. Chem.*, 1986, **51**, 2655–2661; (*c*) R. W. Pipal, K. T. Stout, P. Z. Musacchio, S. Ren, T. J. A. Graham, S. Verhoog, L. Gantert, T. G. Lohith, A. Schmitz, H. S. Lee, D. Hesk, E. D. Hostetler, I. W. Davies and D. W. C. MacMillan, Metallaphotoredox Aryl and Alkyl Radiomethylation for PET Ligand Discovery, *Nature*, 2021, **589**, 542–547.

6 Selected Examples: (*a*) P. Ruiz-Castillo and S. L. Buchwald, Applications of Palladium-Catalyzed C–N Cross-Coupling Reactions, *Chem. Rev.*, 2016, **116**, 12564–12649; (*b*) Z. Chen and M. Brookhart, Exploring Ethylene/Polar Vinyl Monomer Copolymerizations Using Ni and Pd α-Diimine Catalysts, *Acc. Chem. Res.*, 2018, **51**, 1831–1839.

7 Selected examples: (*a*) I. E. Marko, S. Sterin, O. Buisine, G. Mignani, P. Branlard, B. Tinant and J.-P. Declercq, Selective and Efficient Platinum(0)-Carbene Complexes as Hydrosilylation Catalysts, *Science*, 2002, **298**, 204–206; (*b*) R. S. Kim and Y. Surendranath, Electrochemical Reoxidation Enables Continuous Methane-to-Methanol Catalysis with Aqueous Pt Salts, *ACS Cent. Sci.*, 2019, **5**, 1179–1186.

8 Selected examples: (*a*) M. J. Burk, Modular Pholane Ligands in Asymmetric Catalysis, *Acc. Chem. Res.*, 2000, **33**, 363–372; (*b*) N. I. Rinehart, A. J. Kendall and D. R. Tyler, A Universally Applicable Methodology for the Gram-Scale Synthesis of Primary, Secondary, and Tertiary Phosphines, *Organometallics*, 2018, **37**, 182–190; (*c*) D. S. Glueck, Catalytic Asymmetric Synthesis of P-Stereogenic Phosphines: Beyond Precious Metals, *Synlett*, 2021, **32**, 875–884.

9 Selected examples: (*a*) Q. Zhao, G. Meng, S. P. Nolan and M. Szostak, N-Heterocycles Carbene Complexes in C–H Activation, *Chem. Rev.*, 2020, **120**, 1981–2048; (*b*) S. Wurtz and F. Glorius, Surveying Sterically Demanding N-Heterocyclic Carbene Ligands with Restricted Flexibility for Palladium-Catalyzed Cross-Coupling Reactions, *Acc. Chem. Res.*, 2008, **41**, 1523–1533.

10 As an example: D. Seebach, A. K. Beck and A. Heckel, TADDOLs, Their Derivatives, and TADDOL Analogues: Versatile Chiral Auxiliaries, *Angew. Chem., Int. Ed.*, 2001, **40**, 92–138.

11 M. A. Bau, S. Wiesler, S. L. Younas and J. Streuff, Strategies for the Synthesis of Chiral Carbon-Bridged Group IV *ansa*-Metallocenes, *Chem.–Eur. J.*, 2019, **25**, 10531–10545.

12 J. D. Firth, P. O'Brien and L. Ferris, Revisiting the Sparteine Surrogate: Development of a Resolution Route to the (−)-Sparteine Surrogate, *Org. Biomol. Chem.*, 2014, **12**, 9357–9365.

13 P. P. Power, Main-Group Elements as Transition Metals, *Nature*, 2010, **463**, 171–177.

14 K. Lee, A. V. Blake, A. Tanushi, S. M. McCarthy, D. Kim, S. M. Loria, C. M. Donahue, K. D. Spielvogel, J. M. Keith, S. R. Daly and A. T. Radosevich, Validating the Biphilic Hypothesis of Nontrigonal Phosphorus(III) Compounds, *Angew. Chem., Int. Ed.*, 2019, **58**, 6993–6998.

15 W. Zhao, S. M. McCarthy, T. Y. Lai, H. P. Yennawar and A. T. Radosevich, Reversible Intermolecular E–H Oxidative Addition to a Geometrically Deformed and Structurally Dynamic Phosphorous Triamide, *J. Am. Chem. Soc.*, 2014, **136**, 17634–17644.

16 Phosphorus triamide **A** can also perform hydroboration by a different mechanism: Y.-C. Lin, E. Hatzakis, S. M. McCarthy, K. D. Reichl, T.-Y. Lai, H. P. Yennawar and A. T. Radosevich, P–N Cooperative Borane Activation and Catalytic Hydroboration by a Distorted Phosphorous Triamide Platform, *J. Am. Chem. Soc.*, 2017, **139**, 6008–6016.

17 Other strained phosphorus analogues can perform similar additions: T. P. Robinson, D. M. De Rosa, S. Aldridge and J. M. Goicoechea, E–H Bond Activation of Ammonia and Water by a Geometrically Constrained Phosphorus(III) Compound, *Angew. Chem., Int. Ed.*, 2015, **54**, 13758–13763.

18 S. A. Culley and A. J. Arduengo, Synthesis and Structure of the First 10-P-3 Species, *J. Am. Chem. Soc.*, 1984, **106**, 1164–1165.

19 A. J. Arduengo and C. A. Stewart, Low-Coordinate Hypervalent Phosphorus, *Chem. Rev.*, 1994, **94**, 1215–1237.

20 N. L. Dunn, M. Ha and A. T. Radosevich, Main Group Redox Catalysis: Reversible P^{III}/P^{V} Redox Cycling at a Phosphorus Platform, *J. Am. Chem. Soc.*, 2012, **134**, 11330–11333.

21 N.-X.-L. nomenclature, C. W. Perkins, J. C. Martin, A. J. Arduengo, W. Lau, A. Alegria and J. K. Kochi, An Electrically Neutral σ-Sulfuranyl Radical from the Homolysis of a Perester with Neighboring Sulfenyl Sulfur: 9-S-3 Species, *J. Am. Chem. Soc.*, 1980, **102**, 7753–7759.

22 T. A. Albright, J. K. Burdett and M.-H. Whangbo, *Orbital Interactions in Chemistry*, Wiley, New Jersey, 2013.

23 A. Kumar, T. M. Bhatti and A. S. Goldman, Dehydrogenation of Alkanes and Aliphatic Groups by Pincer-Ligated Metal Complexes, *Chem. Rev.*, 2017, **117**, 12357–12384.

24 M. Mediati, G. N. Tachibana and C. M. Jensen, Isolation and Characterization of IrH₂Cl(η²-H₂)[P(*i*-Pr)₃]₂: A Neutral Dihydrogen Complex of Iridium, *Inorg. Chem.*, 1990, **29**, 5–9.

25 (*a*) M. Gupta, C. Hagen, R. J. Flesher, W. C. Kaska and C. M. Jensen, A Highly Active Alkane Dehydrogenation Catalyst: Stabilization of Dihydrido Rhodium and Iridium Complexes by a P–C–P Pincer Ligand, *Chem. Commun.*, 1996, 2083–2084; (*b*) M. Gupta, C. Hagen, W. C. Kaska, R. E. Cramer and C. M. Jensen, Catalytic Dehydrogenation of Cycloalkanes to Arenes by a Dihydrido Iridium P–C–P Pincer Complex, *J. Am. Chem. Soc.*, 1997, **119**, 840–841; (*c*) F. Liu, E. B. Pak, B. Singh, C. M. Jensen and A. S. Goldman, Dehydrogenation of *n*-Alkanes Catalyzed by Iridium "Pincer" Complexes: Regioselective Formation of α-Olefins, *J. Am. Chem. Soc.*, 1999, **121**, 4086–4087.

26 J. Zhao, A. S. Goldman and J. F. Hartwig, Oxidative Addition of Ammonia to Form a Stable Monomeric Amido Hydride Complex, *Science*, 2005, **307**, 1080–1082.

27 A. J. Arduengo, C. A. Stewart, F. Davidson, D. A. Dixon, J. Y. Becker, S. A. Culley and M. B. Mizen, The Synthesis, Structure, and Chemistry of 10–Pn–3 Systems: Tricoordinate Hypervalent Pnictogen Compounds, *J. Am. Chem. Soc.*, 1987, **109**, 627–647.

28 P. Simon, F. de Proft, R. Jambor, A. Ruzicka and L. Dostal, Monomeric Organoantimony(I) and Organobismuth(I) Compounds Stabilized by an NCN Chelating Ligand: Syntheses and Structures, *Angew. Chem., Int. Ed.*, 2010, **49**, 5468–5471.

29 P. Simon, R. Jambor, A. Ruzicka and L. Dostál, Oxidative Addition of Diphenyldichalcogenides PhEEPh (E = S, Se, Te) to Low-Valent CN- and NCN-Chelated Organoantimony and Organobismuth Compounds, *Organometallics*, 2013, **32**, 239–248.

30 S. W. Benson, Thermochemistry and Kinetics of Sulfur-Containing Molecules and Radicals, *Chem. Rev.*, 1978, **78**, 23–35.

31 S. J. Blanksby and G. B. Ellison, Bond Dissociation Energies of Organic Molecules, *Acc. Chem. Res.*, 2003, **36**, 255–263.

32 J. Hyvl, W. Y. Yoshida, A. L. Rheingold, R. P. Hughes and M. F. Cain, A Masked Phosphinidene Trapped in a Fluxional NCN Pincer, *Chem.–Eur. J.*, 2016, **22**, 17562–17565.

33 V. Kremlacek, J. Hyvl, W. Y. Yoshida, A. Ruzicka, A. L. Rheingold, J. Turek, R. P. Hughes, L. Dostal and M. F. Cain, Heterocycles Derived from Generating Monovalent Pnictogens within NCN Pincers and Bidentate NC Chelates: Hypervalency versus Bell-Clappers versus Static Aromatics, *Organometallics*, 2018, **37**, 2481–2490.

34 Related OCO pincers have been prepared: R. Jambor, L. Dostal, A. Ruzicka, I. Cisarova, J. Brus, M. Holcapek and J. Holecek, Organotin(IV) Derivatives of Some O,C,O-Chelating Ligands, *Organometallics*, 2002, **21**, 3996–4004.

35 L. A. van de Kuil, H. Luitjes, D. M. Grove, J. W. Zwikker, J. G. M. van der Linden, A. M. Roelofsen, L. W. Jenneskens, W. Drenth and G. van Koten, Electronic Tuning of Arylnickel(II) Complexes by Para Substitution of the Terdentate Monoanionic 2,6-Bis[(Dimethylamino)methyl]phenyl Ligand, *Organometallics*, 1994, **13**, 468–477.

36 (*a*) J. Vrana, R. Jambor, A. Ruzicka, A. Lycka, F. De Proft and L. Dostal, N→As Intramolecularly Coordinated Organoarsenic(III) Chalcogenides: Isolation of Terminal As–S and As–Se Bonds, *J. Organomet. Chem.*, 2013, **723**, 10–14; (*b*) I. Vranova, R. Jambor, A. Ruzicka, R. Jirasko and L. Dostal, Reactivity of N,C,N-Chelated Antimony(III) and Bismuth(III) Chlorides with Lithium Reagents: Addition vs Substitution, *Organometallics*, 2015, **34**, 534–541; (*c*) L. Dostal, I. Cisarova, R. Jambor, A. Ruzicka, R. Jirasko and J. Holecek, Structural Diversity of Organoantimony(III) and Organobismuth(III) Dihalides Containing O,C,O-Chelating Ligands, *Organometallics*, 2006, **25**, 4366–4373.

37 J. Hyvl, W. Y. Yoshida, C. E. Moore, A. L. Rheingold and M. F. Cain, Unexpected Detours and Reactivity Encountered During the Planned Synthesis of Hypervalent 10–Pn–3 Species (Pn = P or As), *Polyhedron*, 2018, **143**, 99–104.

38 C. N. Smit, Th. A. van der Knapp and F. Bickelhaupt, Stable Unsymmetrical Diphosphenes, *Tetrahedron Lett.*, 1983, **24**, 2031–2034.

39 M. Yoshifuji, I. Shima, N. Inamoto, K. Hirotsu and T. Higuchi, Synthesis and Structure of Bis(2,4,6-tri-*tert*-butylphenyl)diphosphene: Isolation of a True "Phosphobenzene", *J. Am. Chem. Soc.*, 1981, **103**, 4587–4589.

40 A. H. Cowley, J. E. Kilduff, J. G. Lasch, S. K. Mehrotra, N. C. Norman, M. Pakulski, B. R. Whittlesey, J. L. Atwood and W. E. Hunter, Synthesis and Structure of Compounds Containing Double Bonds between the Heavier Group 5A Elements: Diphosphenes, Diarsenes, Phosphaarsenes, and Phosphastibenes, *Inorg. Chem.*, 1984, **23**, 2582–2593.

41 M. H. Holthausen, D. Knackstedt, N. Burford and J. J. Weigand, Phosphenium-Insertion and Chloronium-Addition Reactions Involving the *cyclo*-Phosphanes (*t*-BuP)ₙ (n = 3, 4), *Aust. J. Chem.*, 2013, **66**, 1155–1162.

42 P. R. Hoffman and K. G. Caulton, Conformational Stability and Ring-Size Integrity of Cyclic Polyphosphines, *Inorg. Chem.*, 1975, **14**, 1997–1999.

43 M. Baudler and K. Glinka, Monocyclic and Polycyclic Phosphanes, *Chem. Rev.*, 1993, **93**, 1623–1667.

44 For X-ray structure of [P(*t*-Bu)]₃: J. Hahn, M. Baudler, C. Kruger and Y.-H. Tsay, Beitrage zur Chemie des Phosphors, 116, Kernresonanzspektren und Kristallstruktur von Tri-tert-butyl-cycltriphosphan, *Z. Naturforsch., B*, 1982, **37b**, 797–805.

45 For X-ray structure of [PCH(SiMe₃)₂]₃: P. A. Baldy and J. Estienne, Structure du Tris[bis(trimethylsilyl)methyl]triphosphiranne, *Acta Crystallogr. C*, 1988, **C44**, 747–749.

46 Bonds composed of orbitals that have more s-character are generally shorter: H. A. Bent, An Appraisal of Valence-Bond Structures and Hybridization in Compounds of the First-Row Elements, *Chem. Rev.*, 1961, **61**, 275–311.

47 (*a*) L. M. Salonen, M. Ellermann and F. Diederich, Aromatic Rings in Chemical and Biological Recognition: Energetics

and Structures, *Angew. Chem., Int. Ed.*, 2011, **50**, 4808–4842; (*b*) C. R. Martinez and B. L. Iverson, Rethinking the Term "Pi-Stacking", *Chem. Sci.*, 2012, **3**, 2191–2201.

48 Related trimerizations were observed in phospha-Wittig chemistry: (*a*) S. Shah and J. D. Protasiewicz, 'Phospha-Wittig' Reactions using Isolable Phosphoranylidenephosphines ArP=PR₃ (Ar = 2,6-Mes₂C₆H₃ or 2,4,6-Buᵗ₃C₆H₂), *Chem. Commun.*, 1998, 1585–1586. For a review of this chemistry: (*b*) S. Shah and J. D. Protasiewicz, 'Phospha-Variations' on the Themes of Staudinger and Wittig: Phosphorus Analogs of Wittig Reagents, *Coord. Chem. Rev.*, 2000, **210**, 181–201.

49 Original synthesis was an aryl iodide not bromide: T. T. Nguyen, R. L. Amey and J. C. Martin, Tridentate Ligand Useful in Stabilizing Higher Coordination States of Nonmetallic Elements. An Aryldialkoxydifluoroperiodinane, *J. Org. Chem.*, 1982, **47**, 1024–1027.

50 Y. Imada, T. Kukita, H. Nakano and Y. Yamamoto, Easy Access to Martin's Hypervalent Sulfur Anions toward an Electrode Material for Organic Rechargeable Batteries, *Bull. Chem. Soc. Jpn.*, 2016, **89**, 546–548.

51 J. C. Martin, "Frozen" Transition States: Pentavalent Carbon *et al*, *Science*, 1983, **221**, 509–514.

52 (*a*) T. T. Nguyen, J. C. Martin and A. Dialkoxyarylbrominane, The First Example of an Organic 10–Br–3 Species, *J. Am. Chem. Soc.*, 1980, **102**, 7383–7385; (*b*) I. Sokolovs, N. Mohebbati, R. Francke and E. Suna, Electrochemical Generation of Hypervalent Bromine(III) Compounds, *Angew. Chem., Int. Ed.*, 2021, DOI: 10.1002/anie.202104677.

53 The procedure in ref. 50 was modified slightly: see ESI† for experimental details.

54 J. Mohr, M. Durmaz, E. Irran and M. Oestreich, Tris(5,6,7,8-Tetrafluoronaphthalen-2-yl)borane, a Partially Fluorinated Boron Lewis Acid with Fluorination Distal to the Boron Atom, *Organometallics*, 2014, **33**, 1108–1111.

55 P. Knochel, W. Dohle, N. Gommermann, F. F. Kneisel, F. Kopp, T. Korn, I. Sapountzis and V. A. Vu, Highly Functionalized Organomagnesium Reagents Prepared through Halogen-Metal Exchange, *Angew. Chem., Int. Ed.*, 2003, **42**, 4302–4320.

56 A. Krasovskiy and P. Knochel, A LiCl-Mediated Br/Mg Exchange Reaction for the Preparation of Functionalized Aryl- and Heteroarylmagnesium Compounds from Organic Bromides, *Angew. Chem., Int. Ed.*, 2004, **43**, 3333–3336.

57 L. Dostal, R. Jambor, A. Ruzicka, R. Jirasko, J. Holecek and F. De Proft, OCO and NCO Chelated Derivatives of Heavier Group 15 Elements. Study on Possibility of Cyclization Reaction via Intramolecular Ether Bond Cleavage, *Dalton Trans.*, 2011, **40**, 8922–8934.

58 *MestReNova v14.2.0-26256*, Mestrelab Research S.L., Santiago de Compostela Spain, 2020.

59 F. Mathey, Developing the Chemistry of Monovalent Phosphorus, *Dalton Trans.*, 2007, 1861–1868.

60 F. C. Courchay, J. C. Sworen, I. Ghiviriga, K. A. Abboud and K. B. Wagener, Understanding Structural Isomerization during Ruthenium-Catalyzed Olefin Metathesis: A Deuterium Labeling Study, *Organometallics*, 2006, **25**, 6074–6086.

61 A. A. Kolomeitsev, F. U. Seifert and G.-V. Roeschenthaler, Simple Preparation of Difluorophosphoranes using Anhydrous Zinc and Tetramethylammonium Fluorides, *J. Fluorine Chem.*, 1995, **71**, 47–49.